Toxicology Reports 7 (2020) 1531–1541

Contents lists available at ScienceDirect

Toxicology Reports

journal homepage: www.elsevier.com/locate/toxrep

Crosslink among phosphatidylinositol-3 kinase/Akt, PTEN and STAT-5A signaling pathways post liposomal galactomannan hepatocellular carcinoma therapy

Rehab M. Abdel-Megeed [a,*], Sameh H. Abd El-Alim [b], Azza F. Arafa [a], Azza A. Matloub [c], Abd El Razik H Farrag [d], Asmaa B. Darwish [b], Abdel- Hamid Z. Abdel- Hamid [a], Mai O. Kadry [a]

[a] Therapeutic Chemistry Department, National Research Centre, El-Buhouth St., Cairo, 12622, Egypt
[b] Pharmaceutical Technology Department, National Research Centre, El-Buhouth St., Cairo, 12622, Egypt
[c] Pharmacognosy D Department, National Research Centre, El-Buhouth St., Cairo, 12622, Egypt
[d] Pathology Department, National Research Centre, El-Buhouth St., Cairo, 12622, Egypt

ARTICLE INFO

Keywords:
Hepatocellular carcinoma
Liposomal galactomannan
PI3K/Akt
PTEN
STAT 5A

ABSTRACT

Liposomal drug-delivery systems (LDDs) provide a promising opportunity to precisely target organs, improve drug bioavailability and reduce systemic toxicity. On the other hand, PI_3K/Akt signaling pathways control various intracellular functions including apoptosis, invasion and cell growth. Hyper activation of PI3K and Akt is detected in some types of cancer that posses defect in PTEN. Tracking the crosstalk between PI3K/Akt, PTEN and STAT 5A signaling pathways, in cancer could result in identifying new therapeutic agents. The current study, identified an over view on PI3K/Akt, PTEN and STAT-5A networks, in addition to their biological roles in hepatocellular carcinoma (HCC). In the current study galactomannan was extracted from *Caesalpinia gilliesii* seeds then loaded in liposomes. Liposomes were prepared employing phosphatidyl choline and different concentrations of cholesterol. HCC was then induced in Wistar albino rats followed by liposomal galactomannan (700 ± 100 nm) treatment. Liver enzymes as well as antioxidants were assessed and PI3K/Akt, PTEN and STAT-5A gene expression were investigated. The prepared vesicles revealed entrapment efficiencies ranging from 23.55 to 69.17%, and negative zeta potential values. The optimum formulation revealed spherical morphology as well as diffusion controlled *in vitro* release pattern. Liposomal galactomannan elucidated a significant reduction in liver enzymes and MDA as well as PI3K/Akt, PTEN and STAT 5A gene expression. A significant elevation in GST and GSH were deduced. In conclusion, Liposomal galactomannan revealed a promising candidate for HCC therapy.

1. Introduction

Drug-delivery systems induce a promising opportunity to overpass the obstacle of in effective drug delivery. Numerous DDs, including liposomes (LPs), nano-emulsions, mesoporous silica nanoparticles, carbon nano-tubes, were highly investigated [1]. LPs posses hydrophobic outer shell and hydrophilic inner core, though it can load different types of drugs and increase solubility. LPs membrane flexibility allows sustained drug release. In addition, LPs with particle size less than 200 nm improve accumulation in tumors, due to enhanced permeability and retention effect, contributing to reduced systemic toxicity and enhanced antitumor efficacy. On these basis, the current study selected LPs as nano-carriers to enhance the therapeutic index of Galactomannan against HCC [2–5].

Liposomes are novel carriers of targeting agents. Liposomal structure is similar to that of biofilm in addition to non-toxicity of their membrane

Abbreviations: AFP, α-fetoprotein; Akt, serine/threonine kinase; ALP, alkaline phasphatase; ALT, alanine aminotransferase; AST, aspartate aminotransferase; Bad, Bcl-2-associated death promoter; *C. gilliesii*, *Caesalpinia gilliesii*; CCl4, carbon tetrachloride; DDs, drug-delivery systems; DEN, diethylnitrosamine; FOXO1, fork-head box protein O1; GM, galactomannan; GSH, glutathione; GSK3, glycogen synthase kinase; GST, glutathione S-transferase; HCC, hepatocellular carcinoma; LDDs, liposomal drug-delivery systems; LPs, liposomes; PI3K, phosphoinositide 3-kinase; PIP2, phosphatidylinositol bisphosphate; PIP3, phosphatidylinositol trisphosphate; PTEN, phosphatase and tensin homolog; STAT-5A, signal transducer and activator of transcription-5A; *TEM*, transmission electron microscopy; VS, vesicle size.

* Corresponding author at: Therapeutic Chemistry Department, National Research Centre, El-Buhouth Street, Dokki, Cairo, 12622, Egypt.
E-mail address: rehabzenbaa@gmail.com (R.M. Abdel-Megeed).

https://doi.org/10.1016/j.toxrep.2020.10.018
Received 6 July 2020; Received in revised form 20 October 2020; Accepted 23 October 2020
Available online 5 November 2020

material [1]. Liposomes may be used to improve the stability of drugs in human body [6]. Due to these advantages, liposomes have previously been used as carriers of different anticancer drugs. The advantages of liposomes as carrier systems include straightforward manufacturing processes, thermodynamic stability, and the ability to entrap either lipophilic, hydrophilic or amphiphilic drug molecules. The oil-in-water emulsions are optimal due to a longer shelf-life compared to other nanoparticulate systems as well as having an accepted regulatory status [7].

Liposomes employed in the pharmaceutical field have several advantages in improving the targeted delivery of drugs and decreasing their toxicity and are utilized in the treatment of a variety of human diseases as Alzheimer's disease, arthritis, atherosclerosis and cancer [8]. Their large size prevents the uptake via healthy tissue, so prevent toxicity [9]. The encapsulation of a rapidly cleared drug can improve its lifetime and protect the normally labile therapeutic agent from premature degradation [10].

Protein kinase B (Akt) plays a vital role in regulation of cell death and survival, cell metabolism, growth and apoptosis [11]. Furthermore, PI3K/Akt signaling network plays a pivot role in cancer survival and development. They are involved in cell differentiation, proliferation, survival, motility, and angiogenesis. Activated PI3K phosphorylates the lipid and the crosstalk between PI3K/Akt and JNK pathways activate PIP2 to generate PIP3, which then phosphorylates Akt leading to its activation. Activated Akt phosphorylate Bcl-2-associated death promoter (Bad), GSK3 and fork-head box protein O1 (FOXO1) to regulate cell survival, growth, metabolism and motility [12]. Nowadays cancer therapies are directed to inhibit cell proliferation based on Akt inhibitors to overcome the high degree of similarity between different AKT isoforms that could discover inhibitors with greater specificity, lower toxicity and reduced side-effects [12].

Phosphatase and tensin homolog (PTEN) is a vital tumor suppressor via suppressing PI3K/Akt signaling pathways. Wild-type PTEN dephosphorylate PIP3 back to PIP2, and interfere with the recruitment of Akt to the plasma membrane, contributing to reduced Akt activation. PTEN locates on chromosome 10q23, which is highly susceptible to mutation in human cancers. Mutation or loss of function of *PTEN* is frequent in a wide range of cancers including liver cancer, gastric, lung and ovarian cancer [7,12].

Chronic inflammation is associated with various metabolic disorders. These disorders includes leads numerous diseases such as cancer, diabetes, neurodegenerative diseases and cardiovascular disease. This inflammation is accompanied by the activation of numerous signaling pathways such as STAT3 and STAT-5A. Genetic deletion in hepatic STAT-5A is associated with higher susceptibility to fibrosis, fatty liver disease and cancer. On the other hand, STAT-5A has a protective role in fatty liver-associated with liver cancer; it exerts oncogenic functions in DEN-induced HCC [13].

Natural polysaccharides are obtained from algae, microorganisms, plants, and animals. As a structurally diverse, they possess antioxidant, anti-inflammatory, anti-mutant, anti-diabetic activities and also act as modulators of coagulation activities [14]. One such polysaccharide has been extracted from the seeds of *Caesalpinia gilliesii*, known as galactomannans. *Caesalpinia gilliesii* (*C. gilliesii*) is a shrub in the legume family, Fabaceae (Leguminosae) (Desert bird of paradise). Proteins derived from the seeds of the *C. gilliesii* ameliorate the toxic effects of chronic doses of acetoaminphen [15]. Anticancer activity of *C. gilliesii* seed extracts against liver carcinoma were reported both in *vivo* and in *vitro* studies [16].

The progression in treatment of cancer isn't sufficient to minimize the annual number of deaths. In addition, the currently used drugs are toxic to normal cells. So, there is an urgent need for new effective and safe strategies for cancer therapy. Thus, the present study was designed to validate the effects of galactomannan polysaccharides encapsulated liposome on liver carcinogenesis.

2. Materials and methods

2.1. Chemicals

L-α-Lecithin, (L-α-phosphatidyl choline, PC), from soybean oil and cholesterol, 99 %, (CH) were purchased from Acros organics, Belgium. Diethylnitrosamine (DEN) was purchased from Sigma-Aldrich Co (Steinheim, Germany). Carbon tetrachloride (CCl4) was obtained from El-Gomhorya Company, Cairo, Egypt. Kits used for the determination of liver function and oxidative stress biomarkers (MDA, GST and GSH) were obtained from Randox Company (Antrim-UK). Primers specific for PI3K, AKT, PTEN, and STAT-5A that were used in real time-PCR were purchased from Qiagen (Germany-Helden). All other chemicals are of high analytical grade.

2.2. Plant material

The seeds of *C. gilliesii* (Family: Fabaceae) were collected in April 2015 from Orman Garden, Giza, Egypt.

2.3. Extraction of galactomannan

Seeds of *Caesalpinia gilliesii,* Family Fabaceae (*C. gilliesii*) were extracted as previously reported [16]. Briefly, The seeds were powdered then defatted using dichloromethane then soaked in 80 % ethanol at 70 °C for 15 min and filtered. The residue was soaked in distilled water with continuous shaking at 25 °C. This process was repeated thrice and the combined supernatant was collected, filtered and concentrated under reduced pressure by means of a rotary evaporator. GM was precipitated from the aqueous extract through the addition of absolute ethanol and keeping in refrigerator overnight and GM was then separated by means of centrifugation at 3000 rpm. The precipitate was further dissolved in the minimum amount of distilled water the previous step was repeated once to obtain pure GM. The obtained GM powder was then lyophilized before further use.

2.4. Preparation of galactomannan loaded liposomes

GM loaded liposomes were prepared by the thin film hydration method [17,18]. Briefly, 100 mg of both PC and CH were dissolved in 10 mL chloroform in a 100 mL pear-shaped flask of a rotary evaporator. The flask was then rotated at 55 ± 2 °C for 10 min. The organic solvent was then evaporated under reduced pressure to form a thin lipid film on the wall of the flask. This thin film was then hydrated with 10 mL phosphate buffer (pH 7.4) containing 10 mg GM for the formation of the liposomal suspension.

2.5. Characterization of galactomannan liposomal formulations

2.5.1. Determination of entrapment efficiency

To determine the amount of GM entrapped in liposomes, the un-entrapped GM was separated by cooling centrifugation (7000× g) at -4 °C, for 30 min using a refrigerated centrifuge (Union 32R, Hanil Science Industrial, Korea) [19]. The amount of entrapped GM was determined in the supernatant employing the method reported by Albalasmeh et al. for carbohydrate determination [20]. Briefly, one ml of the supernatant was mixed, after suitable dilution, with 3 mL of concentrated sulfuric acid. The solution was cooled in an ice bath for 2 min then measured spectrophotometrically at 315 nm using a UV spectrophotometer (Shimadzu UV spectrophotometer, 2401/PC, Japan). Blank solution was prepared following the same procedure, using phosphate buffer (pH 7.4). The EE% was calculated by difference from the amount of free, un-entrapped GM using the following equation:

$$EE\% = \frac{\text{Total GM} - \text{Free GM}}{\text{Total GM}} \times 100$$

2.5.2. Determination of vesicle size, polydispersity index and zeta potential

The mean vesicle size (VS) and polydispersity index (PDI) were determined by the photon correlation spectroscopy with a Malvern Zetasizer Nano ZS at an angle of 90″ in 10 mm diameter cells at 25 °C (Malvern Instrument Ltd., Worcestershire, UK). Before measurement, the formulations were diluted appropriately with double distilled water.

Using the same instrument, the ZP of charged vesicles was determined by observing their electrophoretic mobility in an electrical field. ZP measurements were performed in double distilled water with conductivity adjusted to 50 mS/cm using sodium chloride solution (0.9 %, w/v).

2.5.3. Transmission electron microscopy

The morphology of the vesicles of the selected liposomal formulation was characterized by transmission electron microscopy (TEM). One drop of the dispersions was placed onto a carbon-coated copper grid and allowed to dry to a thin film. Before complete drying, the film was stained with 1 % phosphotungstic acid and left to dry at room temperature. The samples were then examined at suitable magnifications by TEM (Jeol, JEM-2100, Tokyo, Japan) with an accelerating voltage of 160 kV.

2.5.4. In-vitro release study

The release of GM from the selected liposomal formulation; L2 was investigated employing the dialysis bag diffusion technique [21]. Cellulose membrane, molecular weight cut off 12,000–14,000, was soaked in phosphate buffer (pH 7.4) for 12 h before use. The bags were filled with an amount of the liposomal formulation equivalent to 2 mg GM and sealed at both ends to avoid leakage. Afterwards, the bags were immersed in screw capped glass containers containing 50 mL phosphate buffer (pH 7.4) and placed in a shaking water bath (Memmert, SV 1422, Germany) rotating at a speed 100 rpm and temperature 37 ± 0.5 °C. Samples were withdrawn at predetermined intervals and replaced with equal volume of freshly phosphate buffer (pH 7.4) to maintain a constant volume. GM concentrations in the withdrawn samples were determined spectrophotometrically at 315 nm as previously mentioned. The cumulative release percentages were calculated as the ratio of the quantity of GM released to the initial quantity instilled in the dialysis bag. The mechanism of GM release was determined using various mathematical models: Zero-order kinetics (cumulative % drug released vs. time), first-order kinetics (log cumulative % drug retained vs. time), higuchi model (cumulative % drug released vs. square root of time).

2.6. In-vivo study

2.6.1. Animals

A total of thirty-two male Wistar rats weighing 150−200 g, were obtained from the animal house of the National Research Center (NRC), Egypt then maintained under standard conditions with a room temperature of 23 ± 5 °C, relative humidity of 50 ± 5% and a 12 h/12 h light/dark cycle. All animals were fed with a standard diet and water. In this study, animals received proper care and handling in compliance with the institutional animal ethics committee of the National Research Centre., Egypt (Approval No. 19075).

Rats were randomly divided into four groups of eight animals each.

Group (1): Animals received normal saline and served as control.

Group (2): HCC-intoxicated animals, DEN was freshly diluted in saline and induced by intrapertioneal injection (200 mg/Kg). Two weeks later, rats received CCl_4 orally (2 mg/Kg) at an equal dilution in corn oil. DEN and CCL_4 were repeated again after one month from the first DEN injection [22].

Group (3): HCC—intoxicated rats were daily treated with the optimized GM encapsulated liposomal formulation intraperitoneally in a dose of 2 mg/Kg for one month [23].

Group (4): HCC—intoxicated rats were daily treated with the optimized GM encapsulated liposomal formulation intraperitoneally in a dose of 4 mg/Kg for one month. The liposomal formulation was suspended in distilled H_2O.

Table 1
Sequence of forward and reverse primers of PI3K, AKT, PTEN, and STAT-5A.

Gene	primer
PI3K	5′-CCA GAC CCT CAC ACT CAG ATCA-3′
	5′-TCC GCT TGG TGG TTT GCT A-3′
AKT	5′-CAT GAA GAG AAG ACA CTG ACC ATG GAAA-3′
	3′-TGG ATA GAG GCT AAG TGT AGA CAC G-5′
PTEN	5′-GGA ACT CCA ACA AGG GAG CA-3′
	5′-TTC GGG GTC GGA AGA CCT TA-3′
STAT-5A	5′-GGG ACA GCC TTT CCT ACT ACC-3′
	5′-GAT CTG CGC AAA AGT CCT GT-3
B-Actin	5′-TGG AGT CTA CTG GCG TCT T-3′
	5′-TGT CAT ATT TCT CGT GGT TCA-3′

2.6.2. Blood and tissue sampling

At the end of the current experiment, rats were anesthetized then blood samples were collected from the sublingual vein and centrifuged at 4000 rpm for 15 min. The obtained sera were kept at −20 °C for biochemical determinations. Rats were sacrificed by cervical dislocation and the liver samples were removed, washed with saline. Then, the liver divided into three portions. The first one was fixed in 10 % phosphate buffered formalin solution for histopathological examination. Another portion was frozen at −80 °C for RNA extraction and gene expression study. The last portion was homogenized in 0.1 M phosphate buffer for biochemical analysis.

2.6.3. Biochemical analysis

Aspartate aminotransferase (AST) and alanine aminotransferase (ALT) were determined by a colorimetric method according to Reitman and Frankel. Serum alkaline phasphatase (ALP) activity was determined by enzymatic colorimetric method according to Belfield and Goldberg [24].

2.6.4. Assays of oxidative stress and antioxidant defense markers

Liver glutathione (GSH) level was estimated using Ellman's reagent [(5, 5-dithiobis-(2-nitrobenzoicacid)] (Biodiagnostic com., Egypt) producing a stable yellow color that measured calorimetrically at 412 nm [25]. Glutathione-S-transferase (GST) activity was determined Glutathione S- Transferase Assay ((Biodiagnostic com., Egypt). Total GST activity (microsomal and cytosolic) was determined by estimating the conjugation of 1-chloro-2,4-dinitrobenzene (CDNB) with reduced glutathione and measured at 340 nm [25,26]. Liver Lipid peroxidation was measured by estimating the levels of malondialdehyde (MDA) using a thiobarbituric acid reaction method [27].

2.6.5. Hepatic α-fetoprotein (AFP) activity

The activity of AFP in serum was assayed using ELISA kits (R &D systems MN, USA) according to the manufacturer's instructions. The assays estimated the quantitative sandwich enzyme immunoassay technique. Specific antibody was pre-coated onto the microplate. The standards, and samples were pipetted into the wells and AFP protein was bound by the immobilized antibody. After washing away any unbound substances, an enzyme-linked secondary antibody specific for AFP was added to the wells. Following color development, the assay was stopped, and the absorbance was read at 450 nm [28].

2.6.6. Quantitative RT-PCR analysis

Total RNA extraction was carried out using Qiqamp mini kit (Qiagen; USA; Cat No. 74104) form liver tissue according to the manufacturer's instructions.

Complementary DNA (cDNA) and mRNA expression of PI3K, AKT, PTEN, and STAT-5A, quantitative real-time PCR were performed using

Table 2
Composition, entrapment efficiency, vesicle size, polydispersity index and zeta potential of GM loaded liposomal formulations.

Formulation code	Amount (mg)		EE% ± SD	VS ± SD	PDI	ZP ± SD
	PC	CH				
L1	100	0	33.05 ± 4.77	651.9 ± 167.1	0.286	−82.4 ± 6.7
L2	90	10	69.17 ± 10.18	678.6 ± 113.7	0.269	−82.0 ± 7.0
L3	80	20	26.87 ± 5.30	758.3 ± 138.2	0.258	−71.0 ± 7.3
L4	70	30	34.18 ± 1.46	391.8 ± 32.8	0.145	−77.3 ± 6.2
L5	60	40	41.61 ± 1.09	737.2 ± 95.4	0.224	−72.8 ± 7.7
L6	50	50	23.55 ± 5.89	855.4 ± 174.9	0.354	−71.4 ± 9.1

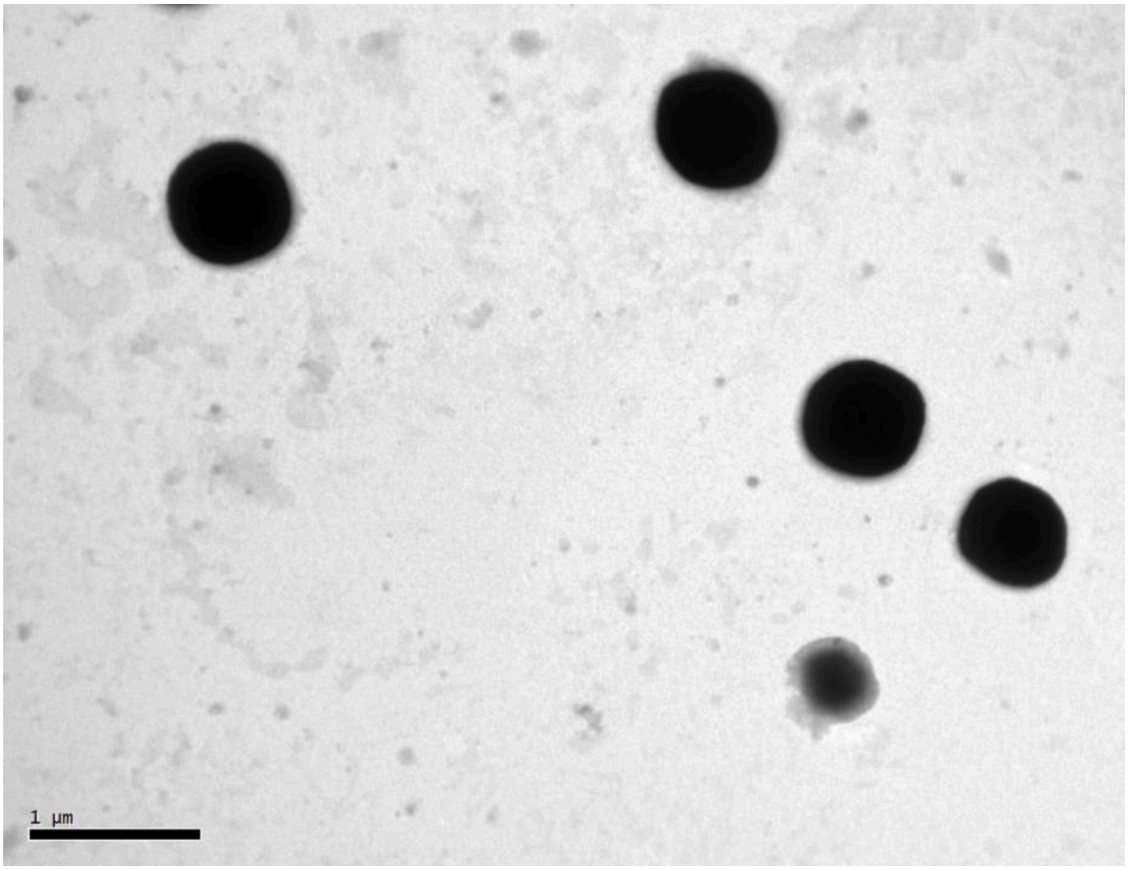

Fig. 1. Transmission electron micrographs of galactomannan loaded liposomal formulation, L-opt.

one step QuantiTecht SYBR green RT-PCR Master Mix (Qiagen; USA; Cat No. 204243). The reaction was run using Stratagene Mx3000 P QPCR System (Agilent Technologies, Santa Clara, CA, USA). Briefly, in a 25 µl reaction volume, 5 µl of cDNA were added to 12.5 µl of 2 × SYBR green Master Mix and 200 ng of each primer. The sequences of primers are described in Table 1. The temperature profile was as follows: 94 °C for 3 min, 94 °C for 20 s,47–57 °C "according to the optimum annealing temperature of each primer" for 20 s and 72 °C for 10 s for 40 cycles. The relative expression of target genes was obtained using comparative CT (ΔΔCT) method [29].

2.6.7. Statistical analysis

Data were expressed as means ± SD. Statistical analysis was carried out using one-way analysis of variance (ANOVA) and Tukey's post HOC test. The level of significance was set at $p < 0.05$.

3. Results

3.1. Preparation of GM loaded liposomes

Six liposomal formulations were prepared in this study using L-α-phosphatidylcholine (PC) as the main lipid. Liposomal vesicles were prepared employing either PC alone or along with different weight ratios of cholesterol. The compositions of the prepared liposomal formulations are presented in Table 2.

3.2. Characterization of GM liposomal formulations

3.2.1. Determination of entrapment efficiency

The EE% of the extract in liposomal formulations is illustrated in Table 2. The results show that the all the prepared vesicles had the ability to entrap GM efficiently, where the EE% ranged from 23.55–69.17 % in all the investigated formulations. The results show that the change in cholesterol ratio had a clear effect on EE%. An increase in the cholesterol content up to 10 % (w/w) led to an obvious increase in EE% whereas further increase from 20 % (w/w) up to 50 %

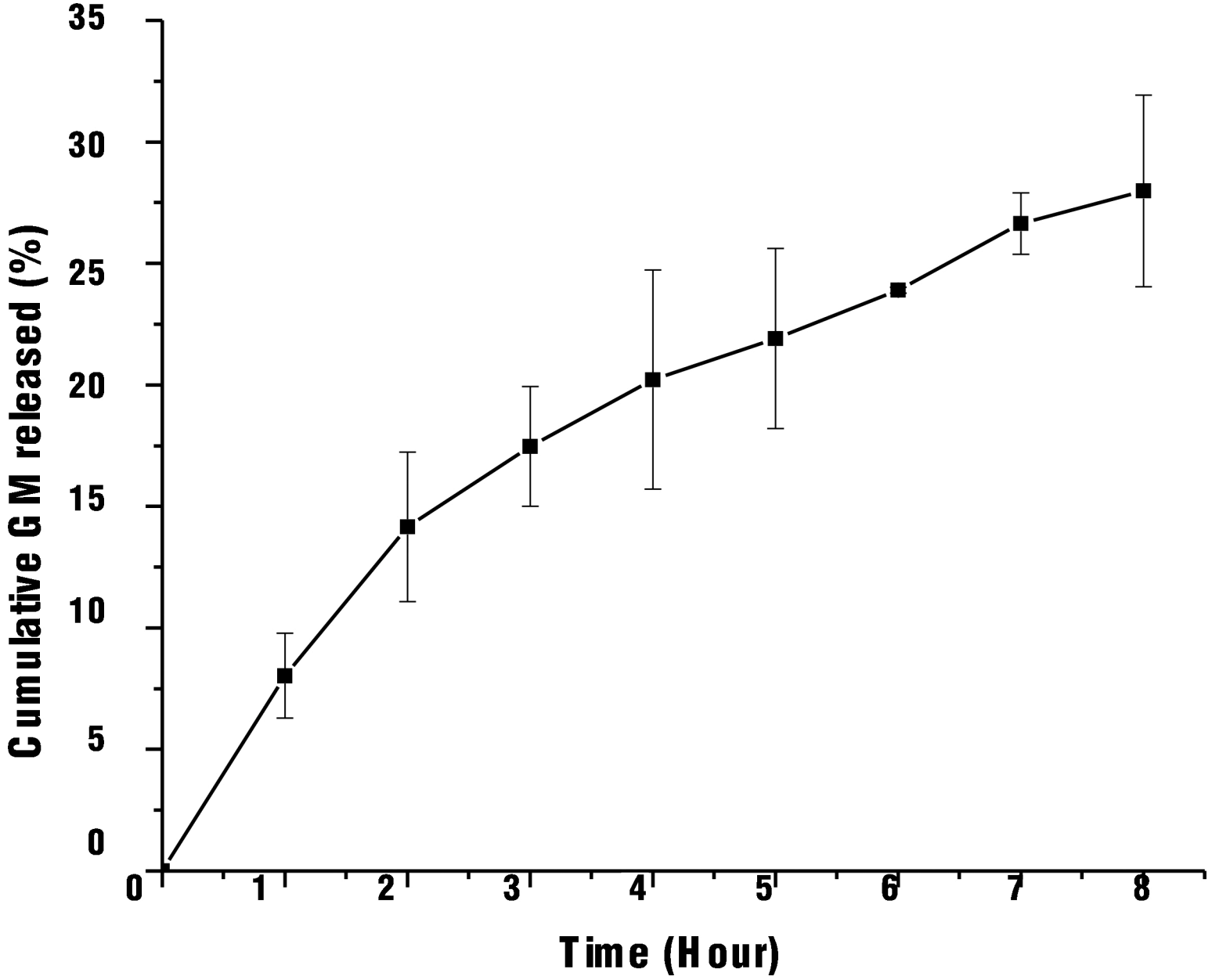

Fig. 2. *In-vitro* release profile of galactomannan loaded liposomal formulation, L-opt.

Table 3
Effect of L-opt on serum level of ALT, AST and ALP on DEN induced liver cancer.

Groups	Parameters		
	AST(U/mL)	ALT(U/mL)	ALP(U/mL)
Control	33.12 ± 2.62[a]	40.31 ± 2.23[a]	154.72 ± 11.23[a]
DEN-intoxicated (% change)	123.89 ± 13.13[b] (274.06%)	158.94 ± 12.97[b] (294.29%)	205.90 ± 17.54[b] (33.08%)
GELs (LD) (% of improvement)	47.84 ± 4.03[c] (299.20%)	54.38 ± 4.87[c] (259.39%)	139.27 ± 12.02[c] (46.94%)
GELs (HD) (% of improvement)	48.98 ± 3.76[c] (226.60%)	58.36 ± 4.95[c] (249.52%)	141.24 ± 12.35[c] (41.79%)

Data were expressed as mean ± SD (n = 8). GELs: galactomannan-encapsulated liposomes, AST: aspartate aminotransferse, ALT: alanine aminotransferase, LD: low dose, HD: High dose.

(w/w) resulted in decreased EE%.

3.2.2. Determination of vesicle size, polydispersity index and zeta potential

The vesicle sizes of the investigated liposomal formulations are presented in Table 2. The prepared formulations showed average vesicle sizes in the nano range (651.9–855.4 nm). PDI values of the prepared formulations ranged from 0.145 to 0.354. Table 2 shows the zeta potential measurements of the investigated liposomal formulations. ZP values ranged from -71.0 to -82.4 mV indicating excellent stability of the niosomal dispersions. In view of the abovementioned results, the liposomal formulation L2 was found to exhibit the highest EE% as well as suitable VS, PDI and ZP values indicating excellent physical stability. Accordingly, this formulation was selected for further investigations and is referred to as L-opt.

3.3. Transmission electron microscopy

Fig. 1 shows TEM micrographs of L-opt. The vesicles are well identified in a nearly perfect sphere to oval shape. Vesicles appear having dark staining, having a smooth surface with no noticeable aggregations or agglomerations.

3.4. In-vitro release study

Fig. 2 depicts the release of GM from L-opt. It could be observed that GM release occurred in two phases. An initial burst release could be observed for the first two hours, where up to 15 % of the drug was

Table 4
Effect of L-opt on some antioxidants levels in DEN induced liver cancer.

Groups	Parameters		
	GSH (mg/g tissue)	GST(U/g tissue)	MDA (nmol/gtissue)
Control	367.35 ± 31.32[a]	839.67 ± 75.36[a]	1005.23 ± 97.51[a]
DEN-intoxicated (% change)	175.29 ± 13.48[b] (-52.28%)	487.06 ± 33.45[b] (-41.99%)	2047.06 ± 102.34[b] (103.64%)
GELs (LD) (% of improvement)	229.81 ± 20.45[c] (14.84%)	596.54 ± 55.67[c] (13.04%)	1026.72 ± 87.91[c] (101.50%)
GELs (HD) (% of improvement)	202.49 ± 17.87[d] (7.40%)	572.55 ± 50.87[d] (10.18%)	1059.19 ± 97.54[d] (98.7%)

Data were expressed as mean ± SD (n = 8). GELs: galactomannan-encapsulated liposomes, GSH: Glutathione, Glutathione- S-Transferase: MD: malondialdehyde, LD: low dose, HD: High dose.

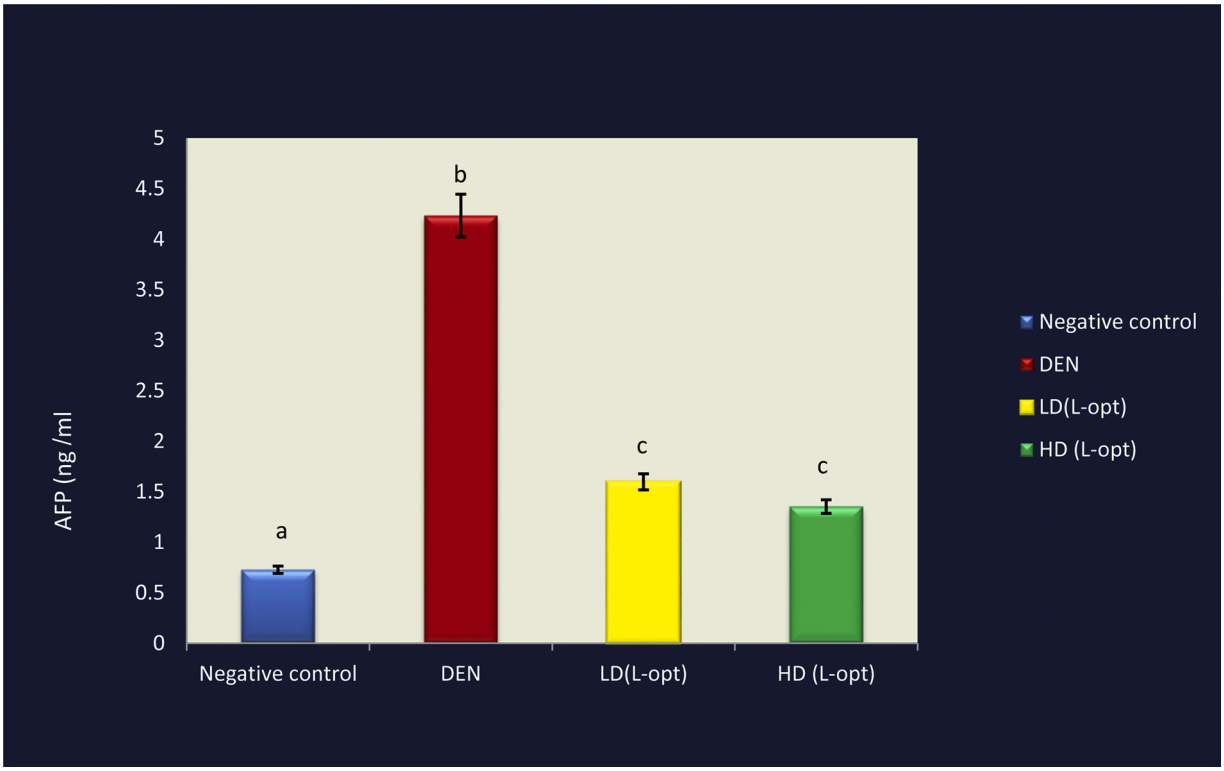

Fig. 3. Effect of L-opt treatment on Serum alpha-fetoprotein level in DEN induced liver cancer. Data are expressed as means ± SEM (n = 10). $p < 0.05$. Groups having different letters are considered significant while Groups having similar letters are considered not significantly different from each other as compared to negative control group.

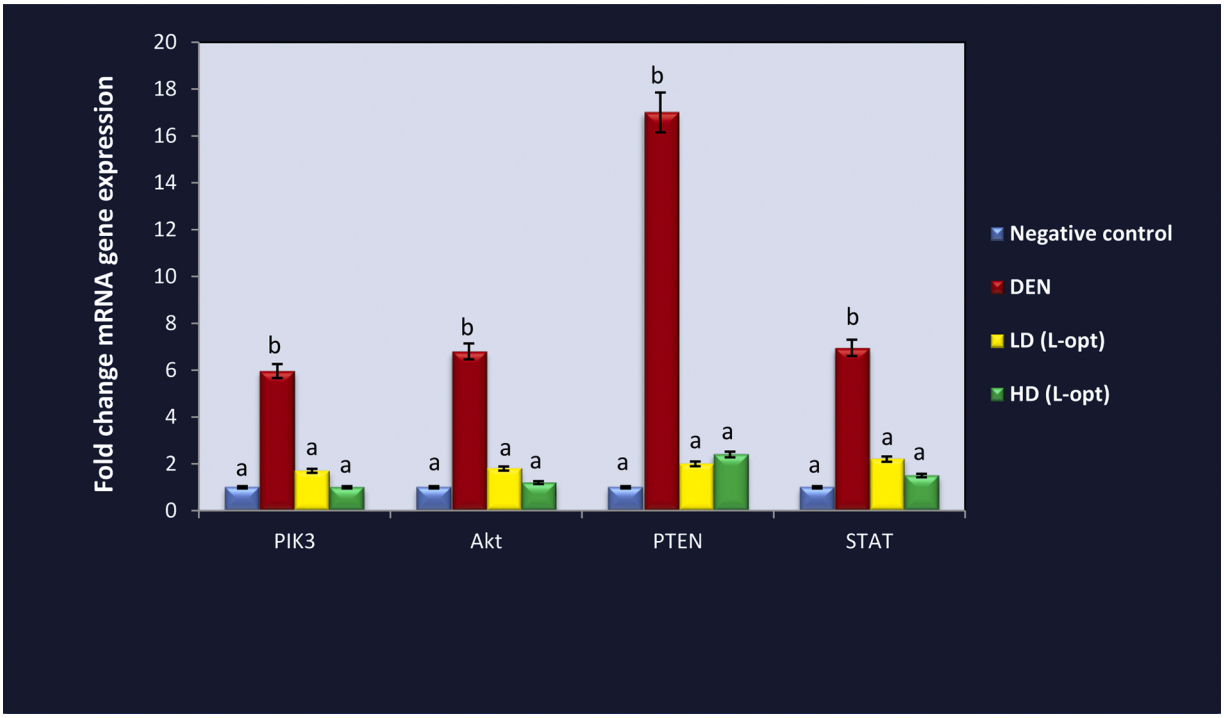

Fig. 4. Effect of L-opt treatment on mRNA gene expression of PIK3, Akt, PTEN and STAT. Data are expressed as means ± SEM (n = 10). $p < 0.05$. Groups having different letters are considered significant while Groups having similar letters are considered not significantly different from each other as compared to negative control group.

released. This is followed by a more sustained release up to hours. In order to determine the release mechanism of GM from liposomal vesicles, linear regression analysis of the mathematical models employed for the release data was performed. Correlation coefficients (R^2) values showed more fitting to Higushi's model ($R^2 = 0.991$) compared to zero order and first order models ($R^2 = 0.954$ and 0.845, respectively).

3.5. In-vivo studies

3.5.1. Effect of liposomal galactomannan on liver enzyme activities

Serum levels of AST, ALT and ALP were significantly increased in DEN intoxicated group by 274.06, 294.29 and 33.08 % relative to the control group. Treatment withL-opt in low dose recorded non-significant percentage of improvements in the activities of these enzymes than that recorded in high dose treatment as compared to the DEN-intoxicated group (Table 3).

3.5.2. Impact of liposomal galactomannan on some antioxidant biomarkers

HCC-intoxicated rats showed significant decrease in GSH and GST levels and significant increase in MDA relative to control group (Table 4). Treatment with L-opt in low and high doses revealed significant elevation in GSH and GST with percentage of improvement reach to 14.84 & 7.40 % for GSH and 13.04 &10.18 for GST, respectively. While, MDA recorded significant reduction in percentage of improvement after treatment withL-opt in both low and high treatment by 101.50 and 98.7 %, respectively as compared to DEN intoxicated group.

3.5.3. Impact of liposomal galactomannan on α-fetoprotein

A significant increase in AFP protein expression was elucidated post DEN intoxication as compared with the control value. Meanwhile, treatment with GELs deduced a significant reduction in AFP with the superiority of the high dose (Fig. 3).

3.5.4. Impact of liposomal galactomannan on PI3K, AKT, PTEN, STAT-5A gene expression

A significant increase in PI3K, AKT, PTEN, STAT-5A gene expression was elucidated post DEN intoxication as compared with the control value. Meanwhile, treatment withL-opt deduced a significant reduction in these genes with the superiority of the high dose (Fig. 4).

3.5.5. Impact of liposomal galactomannan on histopathological architecture

As observed in Fig. 5 (C&D), DEN-intoxicated rat liver showed fibrosis, cirrhosis, encapsulated regenerative nodules, early tumorous nodules. On the other hand Fig. 6 displays group treated with L-opt in low dose (A, B), showing marginal to moderate improvement of hepatic histology whereas group treated with L-opt in high dose (C, D)exhibited near-normal architecture of the hepatic and portal lobules.

4. Discussion

A growing body of evidence indicated that HCC is the third leading cause of cancer deaths globally [30]. It is closely associated with chronic inflammation and fibrosis. The rising incidence of HCC is due to the emergence of hepatitis viral infection, chronic alcohol abuse and the liver pathologies associated with obesity [31].

The sequence of molecular pathogenesis of HCC is complex and 80 % of cirrhotic livers are related to different factors. Different chromosomal aberrations, genetic and epigenetic variations, mutations of gene and alternation in signaling pathways let us to pave the way for knowledge of HCC etiology [32].

In this fact, the present study investigated the therapeutic index of liposomal galactomannan on DEN induced HCC and the crosstalk between PI3K/AKT, PTEN and STAT-5A signaling pathways that may be related to this pathogen.

In the current study, liposomal formulations were prepared employing PC along with CH where several ratios of CH ranging from 0 to 50% (w/w) were investigated. Cholesterol is one of the common

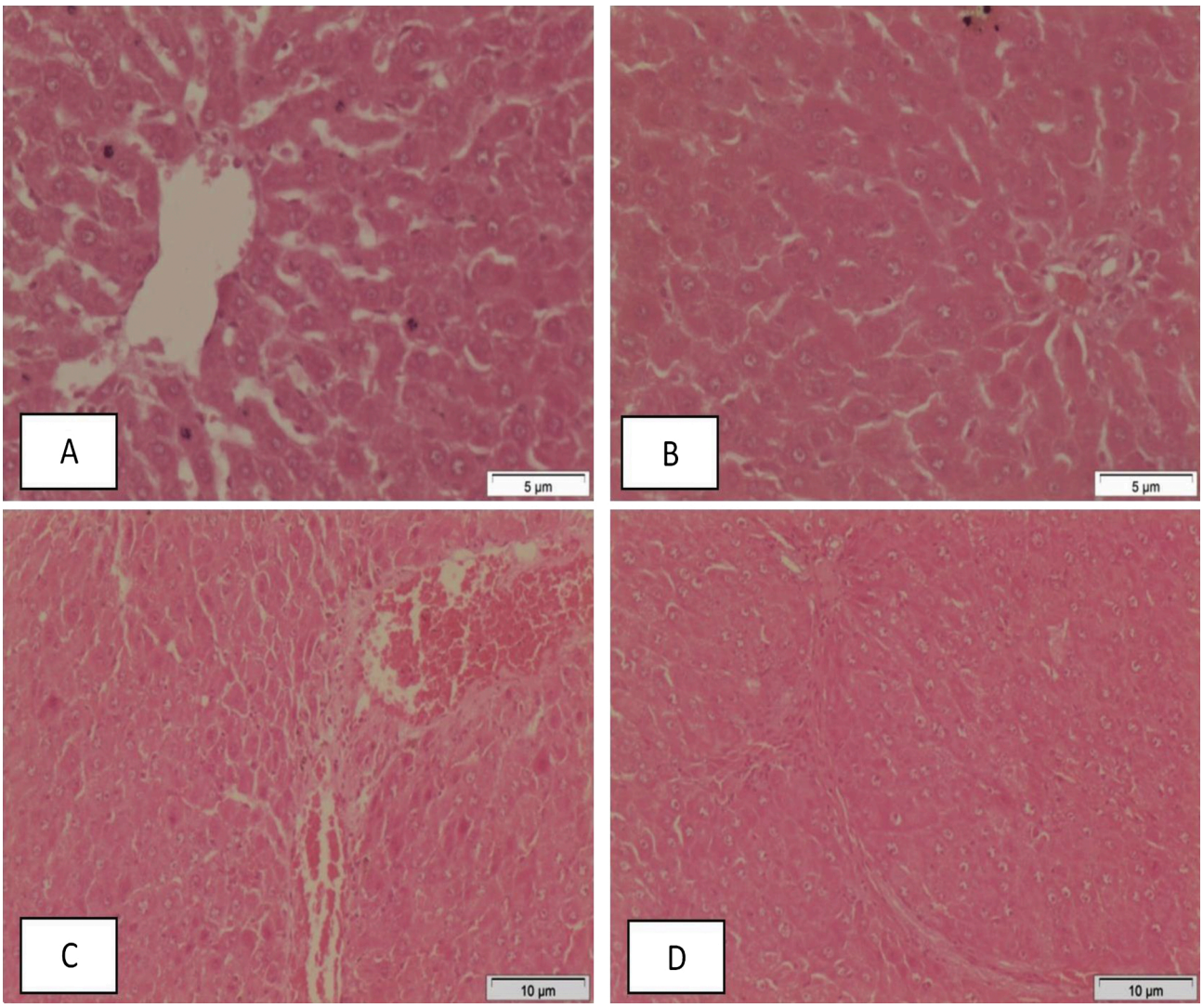

Fig. 5. Micrograph sections of liver of A) control rat shows the normal architecture of hepatic lobule. The central vein lies at the center of the lobule surrounded by cords of hepatocytes. Between the strands of hepatocytes the hepatic sinusoids are shown, B) control liver of rat shows the normal architecture of the portal tract, C) DEN- treated rat liver show significant liver fibrosis occurred and marked atrophy of entrapped hepatocytes, D) DEN- treated rat liver show fibrosis, cirrhosis, encapsulated regenerative nodules, early tumorous nodules (H&E, Scale bar: 10 µm).

additives used in liposomal formulation [33]. Numerous studies have shown that cholesterol can increase the packing of phosphor-lipid molecules [34], change the fluidity of intra-vesicle interactions to make them more rigid and sustain in severe shear stress of the lipid bilayer [35] and instead reduce bilayer permeability [36]. An optimum amount of cholesterol is vital as it represents a good equilibrium between flexibility furnished by lipids and the stability ensured by cholesterol [33]. The initial increase in EE % with the addition of cholesterol could be attributed to an increase in the membrane micro-viscosity by abolishing the gel-to-liquid phase transition of the lipid bilayer, which leads to an increase in hydrophobicity and stability of the bilayer hydrophobicity and stability [37]. On the other hand, further increase in the amount of cholesterol results in a decrease of EE% through competition with the drug for the bilayer, hence hindering the entrapment of the drug into the vesicles [38].

Liposomal multilamellar vesicles (MLV) usually have vesicle sizes greater than 0.1 µm and consist of two or more bilayers [39]. Due to their large size, they are cleared rapidly by the reticulo-endithelial system (RES) cells and hence can be targeted to organs [40]. It can also be noted that there is a general increase in the mean size of liposomes increasing CH content. These results are in accordance with previous reports [41]. All the liposomal formulations exhibited low PDI values (<0.5) indicating homogenous dispersion, suggesting stable and reproducible VSs [42–44]. The negative zeta potential values of the prepared vesicles could be ascribed to the preferential adsorption of hydroxyl ions at the vesicle surface [45,46].This finding has been previously reported in neutral vesicular carriers such as liposomes [43] and niosomes [47].

The release of GM from the liposomal vesicles occurred in two phases [47–49]. The initial burst release could be attributed to the liberation of drug molecules incorporated at the surface and within the liposomal bilayers, thus leading to rapid release upon dispersing niosomes in the release medium [18]. This is followed by a more sustained release as drug liberation becomes regulated by diffusion throughout the swollen liposomal vesicles [50]. Drug release from liposomal formulations follow Higuchi's model of drug release which comes in agreement with previous reports [51,52].

A significant increment in ALT, AST and ALP activities were observed in DEN intoxicated rats relative to the control value. This elevation might be related to the over production of these enzymes, increased cell membrane permeability resulting in spillage of these enzymes to the serum. Elevated liver function tests reflect loss of liver cell

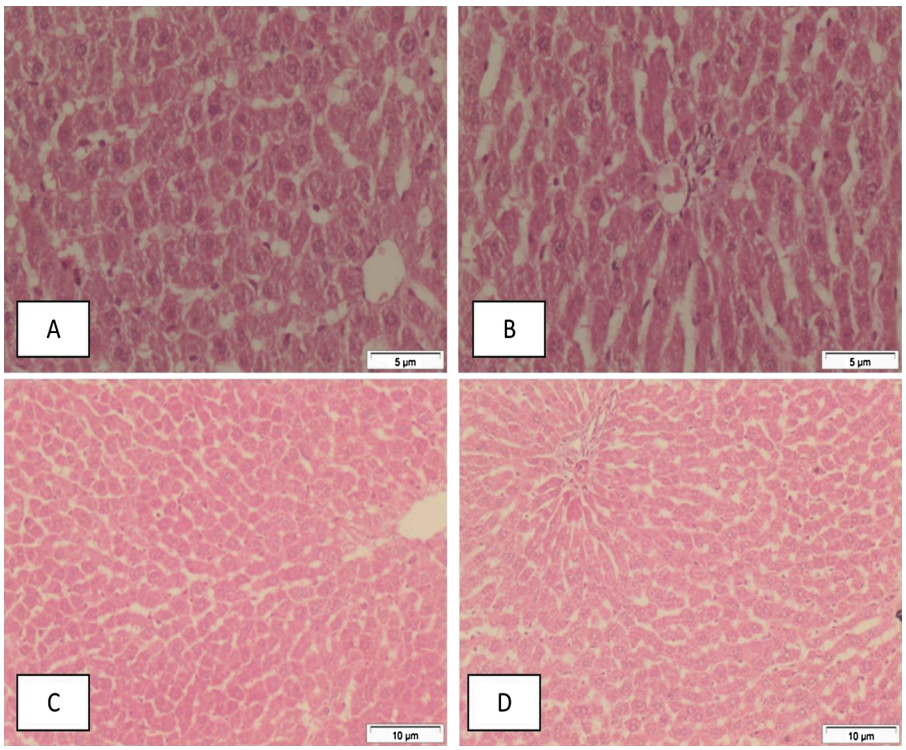

Fig. 6. Micrograph liver sections of L-opt treated groups: Low dose (A, B) and High dose(C, D) show marginal to moderate improvement of hepatic histology. Near-normal architecture of the hepatic and portal lobules was observed (H&E, Scale bar: 10 µm).

membranes integrity and cellular leakage [53]. ALP is closely connected with lipid membrane in canalicular ducts. Therefore, any interference with the bile flow contributes to elevated serum ALP activity [53]. Some studies reported an association between the liver enzymes functions and the risk of HCC development [54]. Meanwhile, treatment with low and high doses of liposomal galactomannan recorded a marked improvement percentage in their activities as compared to DEN-intoxicated group.

Herein, DEN intoxication induced a significant reduction in the activity of GST and GSH content in liver tissue relative to the control value. On the other hand, a significant elevation in MDA level was elucidated in DEN intoxicated rats. Oxidative stress beside the deficiency of antioxidant defense mechanism might be a critical factor contributing to HCC development [55]. This may be also attributed to the hypothesis that DEN enhances cellular injury and oxidative stress via ROS formation. DEN is metabolized in acidic gastric medium to active ethyl radical that causes DNA mutation, contributing to carcinogenesis [29]. This intoxication was ameliorated post liposomal galactomannan treatment in low and high doses with the low dose showing the most significant effect.

A significant up regulation in PI3K, AKT, PTEN and STAT-5A gene expression was elucidated in DEN intoxicated rats relative to the control value. This elevation might be related to that phosphoinositide 3-kinases (PI3Ks) are involved in cell proliferation, motility, survival and intracellular trafficking, which in turn leads to tumor development. AKT was originally identified as the oncogene and it is frequent in a wide range of cancers [56]. It is found in an inactive form then its activation occurs through PI3K. AKT/PI3K signaling network participate in cancer survival and development [11]. PTEN acts as a tumor suppressor gene. It regulates a cell during division, replication and considered as a target of many anticancer drugs. STAT5A gene exerts oncogenic functions in leukemia, breast, colon and prostate cancer [57–60].

The PI3K inhibitors and wild-type PTEN expression are able to inhibit both Akt and JNK activation. Activated c-Jun by JNK binds to the promoter sequence of *PTEN,* resulting in the inhibition of *PTEN* transcription and activation of Akt [61]. Crosstalk between PI3K/Akt and JNK pathways is constitutively active in some types of cancers.

In hepatocytes, growth hormone binding to its receptor (GHR) activates Janus kinase (JAK) 2, which in turn activates signal transducer and activator of transcription (STAT) 5A and STAT5B. Activated STAT5 translocates to the nucleus to regulate genes involved in vital liver functions, including postnatal body growth, cell cycle progression, lipid, bile acid, reactive oxygen species (ROS) and drug metabolism [13]. It was shown that impaired GH-STAT5 signaling correlates with chronic liver disease, i.e. the development of fatty livers is driven by loss of hepatic STAT5 expression changing ROS, glucose and lipid metabolism [13]. In addition, STAT5 deficiency in mice has been associated with higher susceptibility to liver fibrosis and cancer, suggesting that hepatic STAT5 has a protective role in mouse models of chronic liver disease by preventing chronic liver damage and tumorigenesis [62].

Activation of STAT5 was previously investigated in patients with HCCs [63]. In addition, loss of STAT5 activity is associated with higher susceptibility to liver fibrosis and cancer in animal models [13,64]. Deficiency in hepatic STAT5 abolishes p53 activity leading to increased DNA damage, further contributing to early HCC [22].

All these deviated parameters were modulated post liposomal galactomannan treatment this is in harmony with the study that observed that liposomes contain a hydrophobic outer shell and hydrophilic inner core that can carry both hydrophobic and hydrophilic drugs, controlling drug release and improving their solubility. LPs with particle size less than 200 nm can improve accumulation in solid tumors, due to retention effect and enhanced permeability, which leads to reduced systemic toxicity and enhanced antitumor efficacy [4].

The genus *Caesalpinia* belonging to *Caesalpinioideae* (family Fabaceae) are widely used in folk medicine. Different bioactive metabolites as flavonoids, terpenoids, phenolics as well as protein and polysaccharides were isolated from different species of *Caesalpinia.* Genus *Caesalpinia* was also reported to possess anticancer antioxidant, antimicrobial, immunomodulatory, and hepatoprotective properties [16]. Biological activity of polysaccharide has attracted the attention of many researchers as therapeutic agents due to limited toxicity.

Galactomannan, was isolated from the seeds of *Caesalpinia* species, and was observed to have commercial importance as stabilizers of emulsion, pharmaceutical stiffeners, textile, biomedical, food industries and cosmetics. The efficacy of GMann against HCC was reported in our previous study [16,65]. Numerous polysaccharides elucidated antitumor, antioxidant, antimicrobial and immunomodulatory effects. Beta glucans isolated from *C. gilliesii* flowers are the most effective polysaccharides used as anti cancer drug [65].

Meanwhile, treatment with GELS elucidated a significant down regulation in PI3K, AKT, PTEN and STAT-5A gene expression with the superiority of the high dose over the low dose.

Drug loaded liposome has the benefits, of increasing efficacy, therapeutic index, stability of drug via encapsulation. They are also nontoxic and reduce the exposure of sensitive tissues to toxic drug. LPs show a pivot efficacy as drug carriers in cancer therapy [66]. Liposomes are currently employed in the treatment of several cancers [8]. Encapsulation of a rapidly cleared drug leads to a considerable increase in the circulation lifetime of the drug [10] and protects the normally labile therapeutic agent from premature degradation by enzymes in the plasma or from simple hydrolysis [67–69].

5. Conclusion

GELs appeared to be an effective free radical quencher via antioxidant defense mechanism. Also, it could modulate the hepatic pathological alteration from DEN induced hepato-carcinogenesis in rats. These findings were of great importance for the development of new and safe drugs for the treatment of liver cancer and may be a promising for further clinical studies. The result of liposome formulation can thus be a substantial increase in antitumor efficacy when compared to the free drug or standard chemotherapy regimens.

Funding source

Not applicable.

Authors' contributions

Rehab M. Abdel Megeed, Mai O. Kadry and Sameh Abd El-Alim developed theoretical formalism, contributed to the original, revision, and final version of the manuscript in addition to experimental part. Azza Arafa, performed Experimental part and formal analysis on rats, Azza Matloub Extract and prepare Galactomannan and contributed to the original, revision, and final version of the manuscript. GWG contributed to the original version of the manuscript. Assmaa prepared liposomal galactomannan. Abdel Razek Faraag performed histopathlogial examination. Abdel-Hamid A. Z. developed theoretical formalism, contributed to the original, revision

Declaration of Competing Interest

No conflict of interest has been declared.

Acknowledgements

The authors are too grateful to National Research Centre (NRC) for supporting us to complete this research.

References

[1] R.R. Joseph, D.W.N. Tan, M.R.M. Ramon, J.V. Natarajan, R. Agrawal, T.T. Wong, S. S. Venkatraman, Characterization of liposomal carriers for the trans-scleral transport of Ranibizumab, Sci. Rep. 7 (2017) 16803.
[2] G. Barratt, Colloidal drug carriers: achievements and perspectives, Cell. Mol. Life Sci. 60 (2003) 213–217.
[3] A.S. Ulrich, Biophysical aspects of using liposomes as delivery vehicles, Biosci. Rep. 22 (2002) 129–150.
[4] S. Zununi Vahed, R. Salehi, S. Davaran, S. Sharifi, Liposome-based drug co-delivery systems in cancer cells, Mater. Sci. Eng. C Mater. Biol. Appl. 7 (2017) 1327–1341.
[5] W.M. Darwish, N.A. Bayoumi, M.T. El-Kolaly, Laser-responsive liposome for selective tumor targeting of nitazoxanide nanoparticles, Eur. J. Pharm. Sci. 111 (2018) 526–533.
[6] B. Aryasomayajula, G. Salzano, V.P. Torchilin, Multifunctional liposomes, Methods Mol. Biol. 1530 (2017) 41–61.
[7] J. Kleynhansa, D. Elgarb, T. Ebenhanc, J.R. Zeevaarta, A. d, Kotzéb, A. Groblera, A toxicity profile of the Pheroid technology in rodents, Toxicol. Rep. 6 (2019) 940–950.
[8] B. Salehi, D. Calina, A.O. Docea, et al., Curcumin's nanomedicine formulations for therapeutic application in neurological diseases, J. Clin. Med. 9 (2020) 430.
[9] A.O. Docea, D. Calina, A.M. Buga, et al., The effect of silver nanoparticles on antioxidant/pro-oxidant balance in a murine model, Int. J. Mol. Sci. 21 (4) (2020) 1233.
[10] S. Ghosh, S. Ghosh, P.C. Sil, Role of nanostructures in improvising oral medicine, Toxicol. Rep. 6 (2019) 358–368.
[11] G.M. Nitulescu, M. Van De Venter, G.M. Nitulescu, A. Ungurianu, P. Juzenas, Q. Peng, O.T. Olaru, D. Grădinaru, A. Tsatsakis, D. Tsoukalas, D.A. Spandidos, D. Margina, The Akt pathway in oncology therapy and beyond, Int. J. Oncol. 53 (6) (2018) 2319–2331.
[12] G.M. Nitulescu, D. Margina, P. Juzenas, Q. Peng, O.T. Olaru, E. Saloustros, C. Fenga, D.A. Spandidos, M. Libra, A.M. Tsatsakis, Akt inhibitors in cancer treatment: the long journey from drug discovery to clinical use (Review), Int. J. Oncol. 48 (3) (2016) 869–885.
[13] D. Margină, A. Ungurianu, C. Purdel, D. Tsoukalas, E. Sarandi, M. Thanasoula, F. Tekos, R. Mesnage, D. Kouretas, A. Tsatsakis, Chronic inflammation in the context of everyday life: dietary changes as mitigating factors, Int. J. Environ. Res. Public Health 17 (2020) 4135.
[14] J.H. Yu, B.M. Zhu, M. Wickre, G. Riedlinger, W. Chen, A. Hosui, et al., The transcription factors signal transducer and activator of transcription 5A (STAT5A) and STAT5B negatively regulate cell proliferation through the activation of cyclin-dependent kinase inhibitor 2b (Cdkn2b) and Cdkn1a expression, Hepatology 52 (2010) 1808–1818.
[15] I. Wijesekara, R. Pangestuti, S.K. Kim, Biological activities and potential health benefits of sulfated polysaccharides derived from marine algae, Carbohydr. Polym. 84 (2011) 14–21.
[16] M.Z. Rizk, H.F. Aly, D.M. Abo-Elmatty, M.M. Desoky, N. Ibrahim, E.A. Younis, Hepatoprotective effect of Caesalipinia gilliesii and Cajanus cajan proteins against acetaminophen over dose induced hepatic damage, Toxicol. Ind. Health 32 (5) (2016) 877–907.
[17] R.M. Abdel-Megeed, A.R. Hamed, A.A. matloub, M.O. Kadry, A.Z. Abdel-Hamid, Regulation of apoptotic and inflammatory signaling pathways in hepatocellular carcinoma via Caesalpinia gilliesii galactomannan, Mol. Cell. Biochem. (2019) 173–184.
[18] M. Mirzaee, P. Owlia, M.R. Mehrabi, A. Gharib, In vitro bactericidal activity of encapsulated amikacin in liposome, Iran. J. Pathol. 4 (2009) 151–156.
[19] J.H. Zhang, J.B. Zhu, A novel method to prepare liposomes containing amikacin, J. Microencapsulation 16 (1999) 511–516.
[20] M.S. El-Ridy, D.M. Mostafa, A. Shehab, E.A. Nasr, S. Abd El-Alim, Biological evaluation of pyrazinamide liposomes for treatment of Mycobacterium tuberculosis, Int. J. Pharm. 330 (2007) 82–88.
[21] A.A. Albalasmeh, A.A. Berhe, T.A. Ghezzehei, A new method for rapid determination of carbohydrate and total carbon concentrations using UV spectrophotometry, Carbohydr. Polym. 97 (2013) 253–261.
[22] Y.Y. Yang, T.S. Chung, X.L. Bai, W.K. Chan, Effect of preparation conditions on morphology and release profiles of biodegradable polymeric microspheres containing protein fabricated by double-emulsion method, Chem. Eng. Sci. 55 (2000) 2223–2236.
[23] S.K. Hassan, A. Moussa, A.R.K. Farrag, Therapeutic and chemopreventive effect of nanocurcumin against diethylnitrosamine induced hepatocellular carcinoma in rats, Int. J. Pharm. Pharm. Sci. 6 (3) (2014) 54–62.
[24] S. Reitman, S.A. Frankel, Colorimeteric method for the determination of serum glutamic oxaloacetic,glutamic pyruvic transaminases, J Clin. Pathol. 28 (1957) 56–63.
[25] A. Belfield, D.M. Goldberg, Revised assay for serum phenyl phosphatase activity using 4-amino-antipyrine, Enzyme 12 (5) (1971) 561–573.
[26] E. Beutler, O. Duron, B.M. Kefly, Improved method for the determination of blood glutathione, J. Lab. Clin. Med. 61 (5) (1963) 882–888.
[27] W. Habig, M.J. Pabst, Glutathione-S-transferase (human placenta), Methods Enzymol. 249 (1974) 7130–7139.
[28] H. Ohkawa, W. Ohishi, K. Yagi, Assay of lipid peroxides in animal tissues by thiobarbituric acid reaction, Anal. Biochem. 95 (1979) 351–358.
[29] M.Z. Rizk, S.A. Ali, M.O. Kadry, G.I. Fouad, N.N. Kamel, E.A. Younis, S.M. Gouda, C-reactive protein signaling and chromosomal abnormalities in Nanotoxicity induced via different doses of TiO2 (80 nm) boost liver function, Biol. Trace Element Res. (2020) in press.
[30] M.O. Kadry, R.M. Abdel-Megeed, E. El-Meliegy, A.Z. Abdel-Hamid, Crosstalk between GSK-3, c-Fos, NFκB and TNF-α signaling pathways play an ambitious role in Chitosan Nanoparticles cancer therapy, Toxicol. Rep. 5 (2018) 723–727.
[31] V. Hernandez–Gea, S. Tofanin, S.L. Friedman, Role of the microenvironment in the pathogenesis and treatment of hepatocellular carcinoma, Gastroenterology 144 (2013) 512–527.
[32] C. Li, X. Bi, Y. Huang, J. Zhao, Z. Li, J. Zhou, M. Zhang, Z. Huang, H. Zhao, J. Cai, Variants identified by hepatocellular carcinoma and chronic hepatitis B virus

infection susceptibility GWAS associated with survival in HBV-related hepatocellular carcinoma, PLoS One 9 (7) (2014), e101586.
[33] A. Villanueva, P. Newell, D. Chiang, S. Friedman, J.M. LIovet, Genes and signaling pathways involved in the pathogensis of HCC, Semin. Liver Dis. 27 (2007) 55–76.
[34] M.L. Briuglia, C. Rotella, A. McFarlane, D.A. Lamprou, Influence of cholesterol on liposome stability and on in vitro drug release, Drug Deliv. Trans. Res. 5 (2015) 231–242.
[35] R.A. Demel, B. De Kruyff, The function of sterols in membranes, Biochim. Biophys. Acta (BBA) - Rev. Biomembr. 457 (1976) 109–132.
[36] D.Z. Liu, W.Y. Chen, L.M. Tasi, S.P. Yang, Microcalorimetric and shear studies on the effects of cholesterol on the physical stability of lipid vesicles, Colloids Surf. A 172 (2000) 57–67.
[37] D. Papahadjopoulos, K. Jacobson, S. Nir, I. Isac, Phase transitions in phospholipid vesicles Fluorescence polarization and permeability measurements concerning the effect of temperature and cholesterol, Biochim. Biophys. Acta (BBA) – Biomembr. 311 (1973) 330–348.
[38] A. Manosroi, P. Wongtrakul, J. Manosroi, H. Sakai, F. Sugawara, M. Yuasa, M. Abe, Characterization of vesicles prepared with various non-ionic surfactants mixed with cholesterol, Colloids Surf. B 30 (2003) 129–138.
[39] G. Arzani, M. Haeri A. Daeihamed, H. Bakhtiari-Kaboutaraki, S. Dadashzadeh, Niosomal carriers enhance oral bioavailability of carvedilol: effects of bile salt-enriched vesicles and carrier surface charge, Int. J. Nanomd. 10 (2015) 4797–4813.
[40] S. Kalepu, K. Sunilkumar, S. Betha, M. Mohanvarma, Liposomal drug delivery system—a comprehensive review, Int. J. Drug. Dev. Res. 5 (2013) 62–75.
[41] A. Sharma, U.S. Sharma, Liposomes in drug delivery: progress and limitations, Int. J. Pharm. 154 (1997) 123–140.
[42] S.C. Lee, K.E. Lee, J.J. Kim, S.H. Lim, The effect of cholesterol in the liposome bilayer on the stabilization of incorporated retinol, J. Liposome Res. 15 (2005) 157–166.
[43] M. Basha, M.M. AbouSamra, G.A. Awad, S.S. Mansy, A potential antibacterial wound dressing of cefadroxil chitosan nanoparticles in situ gel: fabrication, in vitro optimization and in vivo evaluation, Int. J. Pharm. 544 (2018) 129–140.
[44] S.H. Abd El-Alim, A.A. Kassem, M. Basha, A. Salama, Comparative study of liposomes, ethosomes and transfersomes as carriers for enhancing the transdermal delivery of diflunisal: in vitro and in vivo evaluation, Int. J. Pharm. 563 (2019) 293–303.
[45] S.H. Abd El-Alim, A.A. Kassem, M. Basha, Proniosomes as a novel drug carrier system for buccal delivery of benzocaine, J. Drug. Deliv. Sci. Tech. 24 (2014) 452–458.
[46] S. Moghassemi, E. Parnian, A. Hakamivala, M. Darzianiazizi, M.M. Vardanjani, S. Kashanian, B. Larijani, K. Omidfar, Uptake and transport of insulin across intestinal membrane model using trimethyl chitosan coated insulin niosomes, Mat. Sci. Eng. Res. 46 (2015) 333–340.
[47] V.B. Junyaprasert, V. Teeranachaideekul, T. Supaperm, Effect of charged and non-ionic membrane additives on physicochemical properties and stability of niosomes, AAPS PharmSciTech 9 (2008) 851–859.
[48] A.A. Kassem, S.H. Abd El-Alim, M.H. Asfour, Enhancement of 8-methoxypsoralen topical delivery via nanosized niosomal vesicles: formulation development, in vitro and in vivo evaluation of skin deposition, Int. J. Pharm. 517 (2017) 256–268.
[49] G.V. Betageri, D.L. Parsons, Drug encapsulation and release from multilamellar and unilamellar liposomes, Int. J. Pharm. 81 (1992) 235–241.
[50] N.K.J.A. Namdeo, Niosomal delivery of 5-fluorouracil, J. Microencapsul. 16 (1999) 731–740.
[51] A. Abd-Elbary, H.M. El-laithy, M.I. Tadros, Sucrose stearate-based proniosome-derived niosomes for the nebulisable delivery of cromolyn sodium, Int. J. Pharm. 357 (2008) 189–198.
[52] M.S. El-Ridy, A.E.A. El-Shamy, A. Ramadan, R.F. Abdel-Rahman, G.A. Awad, A. El-Batal, A.M. Mohsen, A.B. Darwish, Liposomal encapsulation of amikacin sulphate for optimizing its efficacy and safety, B. J. Pharm. Res. 5 (2015) 98.
[53] M. El-Badry, G. Fetih, F. Shakeel, Comparative topical delivery of antifungal drug croconazole using liposome and micro-emulsion-based gel formulations, Drug Deliv. 21 (2014) 34–43.
[54] J. Zhao, L. Peng, C. Geng, Y.P. Liu, Wang Xu, H.C. Yang, S.J. Wang, Preventive effect of hydrazinocurcumin on carcinogenesis of diethylnitrosamine-induced hepatocarcinoma in male SD Rats, Asian Pac. J. Cancer Prev. 15 (2014) 2115–2121.
[55] N. Kadasa, H. Fabdalla, M. Afifi, S.G. Gowayed, Hepatoprotective effects of curcumin against diethyl nitrosamine induced hepatotoxicity in albino rats, Asian Pac. J. Cancer Prev. 16 (1) (2015) 103–108.
[56] S. Cheng, P. Lin, H. Liu, Y. Peng, S. Huang, Y. Huang, VitaminB-6 supplementation could mediate antioxidant capacity by reducing plasma homocysteine concentration in patients with hepatocellular carcinoma after tumor resection, Bio. Med. Res. Int. (2016) 1–7.
[57] D.A. Garcia-Dios, D. Lambrechts, L. Coenegrachts, I. Vandenput, A. Capoen, P. M. Webb, K. Ferguson, et al., High-throughput interrogation of PIK3CA, PTEN, KRAS, FBXW7 and TP53 mutations in primary endometrial carcinoma, Gynecol. Oncol. 128 (2013) 327–334.
[58] P. Kar, P.C. Supakar, Expression of Stat5A in tobacco chewing-mediated oral squamous cell carcinoma, Cancer Lett. 28 (2) (2006) 306–311, 240.
[59] Y. Liao, X. Hu, X. Huang, C. He, Quantitative analyses of CD133 expression facilitate researches on tumor stem cells, Biol. Pharm. Bull. 33 (5) (2010) 738–742.
[60] A.R. Peck, A.K. Witkiewicz, C. Liu, A.C. Klimowicz, G.A. Stringer, E. Pequignot, et al., Low levels of Stat5a protein in breast cancer are associated with tumor progression and unfavorable clinical outcomes, Breast Cancer Res. 14 (5) (2012) R130.
[61] X. Hong, G. Chen, M. Wang, C. Lou, Y. Mao, Z. Li, Y. Zhang, STAT5a-targeting miRNA enhances chemosensitivity to cisplatin and 5-fluorouracil in human colorectal cancer cells, Mol. Med. Rep. 5 (5) (2012) 1215–1219.
[62] M. Zhao, X.F. Ding, J.Y. Shen, X.P. Zhang, X.W. Ding, B. Xu, Use of liposomal doxorubicin for adjuvant chemotherapy of breast cancer in clinical practice, J. Zhejiang Univ. Sci. B 18 (2017) 15–26.
[63] K.M. Mueller, J.W. Kornfeld, K. Friedbichler, L. Blaas, G. Egger, H. Esterbauer, et al., Impairment of hepatic growth hormone and glucocorticoid receptor signaling causes steatosis and hepatocellular carcinoma in mice, Hepatology 54 (2011) 1398–1409.
[64] T.K. Lee, K. Man, R.T. Poon, C.M. Lo, A.P. Yuen, I.O. Ng, et al., Signal transducers and activators of transcription 5b activation enhances hepatocellular carcinoma aggressiveness through induction of epithelial-mesenchymal transition, Cancer Res. 66 (2006) 9948–9956.
[65] S.Y. Shi, C.T. Luk, S.A. Schroer, M.J. Kim, D.W. Dodington, T. Sivasubramaniyam, et al., Janus Kinase 2 (JAK2) dissociates hepatosteatosis from hepatocellular carcinoma in mice, J. Biol. Chem. 292 (2017) 3789–3799.
[66] V. Vetvicka, J. Vetvickova, β 1,3 in cancer treatment, Am. J. Immunol. 2 (2012) 38–43.
[67] J.L. Arias, B. Clares, M.E. Morales, V. Gallardo, M.A. Ruiz, Lipid-based drug delivery systems for cancer treatment, Curr. Drug Targets 12 (8) (2011) 1151–1165.
[68] J. Stefanowicz-Hajduk, J.R. Ochocka, Real-time cell analysis system in cytotoxicity applications: usefulness and comparison with tetrazolium salt assays, Toxicol. Rep. 7 (2020) 335–344.
[69] M. Slingerland, H.J. Guchelaar, H. Gelderblom, Liposomal drug formulations in cancer therapy: 15 years along the road, Drug Discov. Today 17 (2017) 160–166.